ARL-TR-9713 • June 2023

Minimum Phase Behavior of High-Speed Tail-Controlled Projectiles

by Tristan D Griffith, John Zelina, Joshua T Bryson, and Benjamin C Gruenwald

NOTICES

Disclaimers

The findings in this report are not to be construed as an official Department of the Army position unless so designated by other authorized documents.

Citation of manufacturer's or trade names does not constitute an official endorsement or approval of the use thereof.

Destroy this report when it is no longer needed. Do not return it to the originator.

ARL-TR-9713 ● JUNE 2023

Minimum Phase Behavior of High-Speed Tail-Controlled Projectiles

Tristan D Griffith
Texas A&M University

John Zelina
Embry-Riddle Aeronautical University

Joshua T Bryson and Benjamin C Gruenwald
DEVCOM Army Research Laboratory

REPORT DOCUMENTATION PAGE	*Form Approved* *OMB No. 0704-0188*

1. REPORT DATE *(DD-MM-YYYY)*
June 2023

2. REPORT TYPE
Technical Report

3. DATES COVERED (From - To)
1 June–16 September 2022

4. TITLE AND SUBTITLE
Minimum Phase Behavior of High-Speed Tail-Controlled Projectiles

5a. CONTRACT NUMBER

5b. GRANT NUMBER

5c. PROGRAM ELEMENT NUMBER

6. AUTHOR(S)
Tristan D Griffith, John Zelina, Joshua T Bryson, and Benjamin C Gruenwald

5d. PROJECT NUMBER

5e. TASK NUMBER

5f. WORK UNIT NUMBER

7. PERFORMING ORGANIZATION NAME(S) AND ADDRESS(ES)
DEVCOM Army Research Laboratory
ATTN: FCDD-RLA-WD
Aberdeen Proving Ground, MD 21005

8. PERFORMING ORGANIZATION REPORT NUMBER
ARL-TR-9713

9. SPONSORING/MONITORING AGENCY NAME(S) AND ADDRESS(ES)

10. SPONSOR/MONITOR'S ACRONYM(S)

11. SPONSOR/MONITOR'S REPORT NUMBER(S)

12. DISTRIBUTION/AVAILABILITY STATEMENT
DISTRIBUTION STATEMENT A. Approved for public release; distribution is unlimited.

13. SUPPLEMENTARY NOTES
primary author's email: <joshua.t.bryson.civ@army.mil>.
ORCID: Joshua Bryson, 0000-0002-0753-6823; Benjamin Gruenwald, 0000-0003-3968-5070

14. ABSTRACT
Tail-controlled projectiles are known to have unstable transmission zeros. Adaptive control architectures and many other control strategies require the transmission zeros be stable to produce stability proofs. Accordingly, many control techniques may not be immediately applied to tail-controlled projectiles. This work presents an overview of the theoretical considerations for the stabilization of transmission zeros by leaking or blending some of the other plant states into the system output. A variety of solutions are presented, but it is ultimately shown that this approach is not worth further exploration because it requires feedback of many more plant states for successful implementation that may not be available for estimation.

15. SUBJECT TERMS flight control, nonminimum phase systems, tail-control, dynamic inversion, adaptive control, guided projectile, high-speed projectile, Weapons Sciences

16. SECURITY CLASSIFICATION OF:			17. LIMITATION OF ABSTRACT	18. NUMBER OF PAGES	19a. NAME OF RESPONSIBLE PERSON
a. REPORT	b. ABSTRACT	c. THIS PAGE			Joshua T Bryson
Unclassified	Unclassified	Unclassified	UU	42	19b. TELEPHONE NUMBER (Include area code) 410-306-1939

Standard Form 298 (Rev. 8/98)
Prescribed by ANSI Std. Z39.18

Contents

List of Figures

List of Tables

1. Introduction

Tail-controlled projectiles present a variety of engineering challenges due to uncertainty in the aerodynamic models, limited control authority, and a lack of redundant systems driven by a need for high performance and reliability at the lowest possible cost. This is further compounded for high-speed projectiles, whose dynamics are nonlinear and whose flight envelopes increasingly include both subsonic and supersonic airspeeds.

Adaptive control schemes have attracted much attention for the autopilot of high-speed projectiles.[1,2] However, it is known that tail-controlled projectiles are nonminimum phase systems. As we show in this work, nonminimum phase systems are not guaranteed to dissipate their internal energy. Stability guarantees for many adaptive control schemes rely on dissipativity as a property of the internal dynamics, so we cannot bolt on existing adaptive controllers to a nonminimum phase system and maintain stability guarantees. This work aims to present a theoretical treatment of nonminimum phase tail-controlled projectiles, modifying the dynamics so that existing adaptive schemes may be readily applied.

A number of strategies have been proposed for treating dynamical systems that are nonminimum phase.[3–6] The most widely discussed and implemented solution is to control a redefined output, which is often a transformation of the body acceleration into a blend of body angles and acceleration that does exhibit minimum phase dynamics.[7]

2. Positive Real Systems

In the study and control of dynamical systems, understanding how energy is stored in the system is important. In the most general sense, a dynamical system that can store up energy and suddenly release it will be more difficult to control than a dynamical system that maintains or decreases its energy. The terms positive real (PR) or strictly positive real (SPR) are used to describe linear systems that maintain or decrease their energy only. Dissipativity is generally reserved for nonlinear systems that that maintain or decrease their energy only.

The PR property allows much stronger mathematical guarantees of stability, so a great deal of literature treats the analysis and control of PR systems.[4,8,9] Consider the following controllable and observable linear continuous-time square system

$$\begin{aligned} \dot{x} &= Ax + Bu \\ y &= Cx. \end{aligned} \tag{1}$$

From Anderson and Vongpanitlerd,[10] the system described by Eq. 1 is PR when

$$\exists P > 0 \ni \begin{cases} A^T P + PA = -Q \leq 0 \\ PB = C^T. \end{cases}$$

There is little controversy over the definition of a PR system. SPR definitions generate more discussion, but here we employ the definition which meets the Kalman-Yacubovich conditions[11]

$$\exists P > 0 \ni \begin{cases} A^T P + PA = -Q < 0 \\ PB = C^T. \end{cases}$$

A particular topic of interest has been the use of (static) output feedback to make a system PR or SPR

$$u = Gy. \tag{2}$$

Using output feedback to make a system PR has the double benefit of controlling the system and providing the stronger guarantees of stability. Dynamical systems which may be made PR with output feedback are called almost positive real (aPR) and dynamical systems that may be made almost SPR with output feedback are called almost strictly positive real (aSPR).[12,13]

We now present the result from Balas and Fuentes[14] that demonstrates a concise test for aSPR systems.

Theorem 1. (A, B, C) *is almost SPR with the control law given by Eq. 2 if and only if the high-frequency gain* CB *is positive definite and the open loop system is minimum phase.*

It should not come as a huge surprise that this result requires the open loop system to be minimum phase. Minimum phase systems have all their transmission (or blocking) zeros in the left-half plane. Intuitively, this results in system dynamics that respond to control commands in a "right way first" manner (see Fig. 1). Conversely, nonminimum phase systems respond in a "wrong way first" manner.

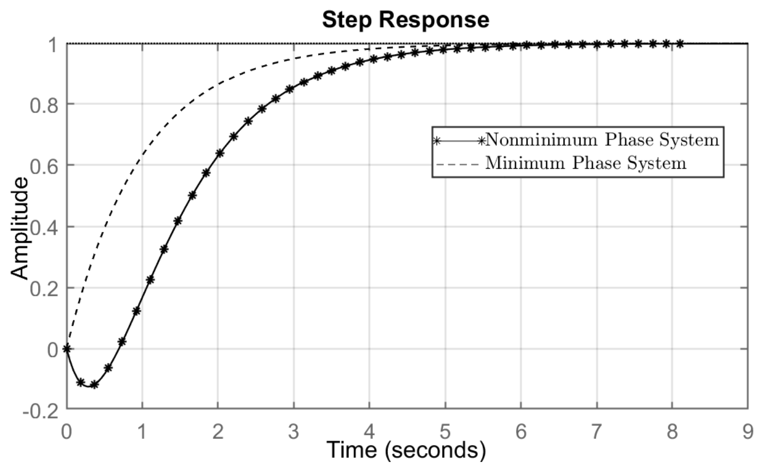

Fig. 1 Step response comparison between a minimum and nonminimum phase system. Note that the minimum phase system immediately heads in the positive direction of the positive step command, while the nonminimum phase system first moves in the negative direction.

Theorem 1 is important for adaptive control techniques, which almost always make use of the aSPR property to prove stability via Lyapunov analysis.[15–17] A particularly aggressive static controller or adaptive controller will note the "wrong way first" response to a command, which increases the tracking error causing the controller to command a greater response. This results in further "wrong way first" responses and can quickly become unstable. Adaptive control techniques are most readily applied to aSPR or SPR systems, although there are techniques for controlling and analyzing nonminimum phase dynamical systems with adaptive control.[18,19]

Notice, the restriction on CB can be somewhat onerous. Positive definiteness implies a square CB with all eigenvalues positive. In particular, this restricts our almost SPR systems to those with the same number of inputs as outputs. While there is some developing theory on the removal of this restriction,[20,21] it remains an obstacle to the theoretical stability of adaptive systems.

With this overview complete, we turn to an introduction of the relevant dynamics for tail-controlled projectiles in order to analyze their positive realness. If these dynamics can be shown or modified to aSPR, a variety of control architectures, adaptive and otherwise, immediately become available as bolt-on solutions with theoretical stability guarantees.

3. Projectile Flight Dynamics

In this section, we provide a brief overview of the nonlinear flight dynamics for a generic tail-controlled projectile. The content presented here can also be found in Griffith et al.[22] with further details given in Bryson and Gruenwald.[23] We include it here to keep the paper self-contained. We begin by noting the relevant reference frames and coordinate systems needed to describe the position and orientation of the projectile. As shown in Fig. 2, the earth reference frame is used as the inertial frame located at the launch location with the x-axis pointing toward the target and the body-fixed reference frame is fixed at the center-of-gravity location on the body of the projectile.

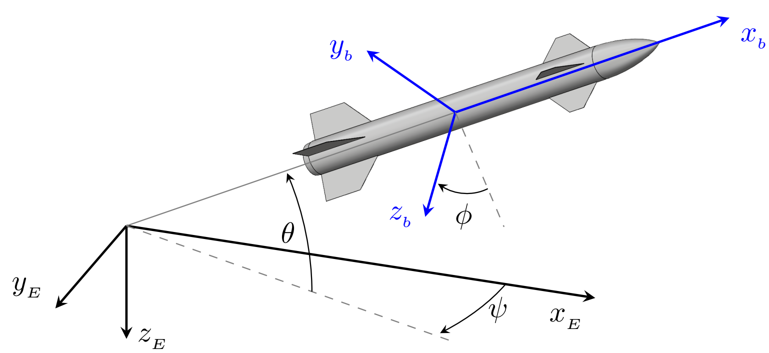

Fig. 2 Illustration of a generic projectile with a body-fixed frame relative to an earth reference frame (inertial frame)

The orientation of the body-fixed frame can be given with respect to the fixed earth reference frame using a ZYX Euler sequence of rotations, where the three Euler angles for roll, pitch, and yaw, are given by ϕ, θ, and ψ, respectively. Using this transformation, the kinematic equations for translational velocity can be given as

$$\begin{bmatrix} \dot{x} \\ \dot{y} \\ \dot{z} \end{bmatrix} = \begin{bmatrix} \mathrm{c}_\theta \mathrm{c}_\psi & \mathrm{s}_\phi \mathrm{s}_\theta \mathrm{c}_\psi - \mathrm{c}_\phi \mathrm{s}_\psi & \mathrm{c}_\phi \mathrm{s}_\theta \mathrm{c}_\psi + \mathrm{s}_\phi \mathrm{s}_\psi \\ \mathrm{c}_\theta \mathrm{s}_\psi & \mathrm{s}_\phi \mathrm{s}_\theta \mathrm{s}_\psi + \mathrm{c}_\phi \mathrm{c}_\psi & \mathrm{c}_\phi \mathrm{s}_\theta \mathrm{s}_\psi - \mathrm{s}_\phi \mathrm{c}_\psi \\ -\mathrm{s}_\theta & \mathrm{s}_\phi \mathrm{c}_\theta & \mathrm{c}_\phi \mathrm{c}_\theta \end{bmatrix} \begin{bmatrix} u \\ v \\ w \end{bmatrix}, \tag{3}$$

where $\mathrm{s}_\phi = \sin(\phi)$, $\mathrm{c}_\phi = \cos(\phi)$, and so forth, the states $[x, y, z]^{\mathrm{T}}$ are the center-of-gravity positions relative to the earth inertial frame, and $[u, v, w]^{\mathrm{T}}$ are the body-fixed translational velocities.

The dynamics of the Euler angles can be described by the body-fixed angular rates as the following kinematic equations

$$\begin{bmatrix} \dot{\phi} \\ \dot{\theta} \\ \dot{\psi} \end{bmatrix} = \begin{bmatrix} 1 & \mathrm{s}_\phi \mathrm{t}_\theta & \mathrm{c}_\phi \mathrm{t}_\theta \\ 0 & \mathrm{c}_\phi & -\mathrm{s}_\phi \\ 0 & \mathrm{s}_\phi/\mathrm{c}_\theta & \mathrm{c}_\phi/\mathrm{c}_\theta \end{bmatrix} \begin{bmatrix} p \\ q \\ r \end{bmatrix}, \tag{4}$$

where $[p, q, r]^\mathrm{T}$ are the body-fixed angular rates acting in the roll, pitch, and yaw planes, respectively, and $\mathrm{t}_\theta = \tan(\theta)$.

The projectile flight dynamics are based on the standard rigid body 6-degree-of-freedom equations of motion. The three translational degrees of freedom are governed by Newton's second law and described by the body-fixed translational velocities given by

$$\begin{bmatrix} \dot{u} \\ \dot{v} \\ \dot{w} \end{bmatrix} = \frac{1}{m} \begin{bmatrix} F_X - mg\mathrm{s}_\theta \\ F_Y + mg\mathrm{s}_\phi \mathrm{c}_\theta \\ F_Z + mg\mathrm{c}_\phi \mathrm{c}_\theta \end{bmatrix} - \begin{bmatrix} 0 & -r & q \\ r & 0 & -p \\ -q & p & 0 \end{bmatrix} \begin{bmatrix} u \\ v \\ w \end{bmatrix}. \tag{5}$$

Here m is the mass of the projectile, g is the gravitational acceleration, and F_X, F_Y, and F_Z are the aerodynamic forces acting on the projectile body in the x, y, and z direction, respectively. The three rotational degrees of freedom are governed by Euler's law and described by the body-fixed angular rates given by

$$\begin{bmatrix} \dot{p} \\ \dot{q} \\ \dot{r} \end{bmatrix} = \begin{bmatrix} I_x^{-1} & 0 & 0 \\ 0 & I_y^{-1} & 0 \\ 0 & 0 & I_z^{-1} \end{bmatrix} \begin{bmatrix} M_l \\ M_m \\ M_n \end{bmatrix} + \begin{bmatrix} I_x^{-1}(I_y - I_z)qr \\ I_y^{-1}(I_z - I_x)pr \\ I_z^{-1}(I_x - I_y)pq \end{bmatrix}, \tag{6}$$

where I_x, I_y, and I_z are the components of inertia around the x, y, and z axes, and M_l, M_m, and M_n are the external moment components resulting from the aerodynamic moments. The inertia matrix is considered to be diagonal with no cross-coupling owing to the symmetric nature of the considered projectile bodies.

Now we introduce the wind reference frame, depicted in Fig. 3, which is defined by the instantaneous orientation of the relative wind velocity vector, denoted as

$\vec{V} \equiv \vec{V}_{CG/E}$, with respect to the body-fixed frame. The relationship between the wind frame and the body-fixed frame is made through the aerodynamic angles: angle of attack, α, and angle of sideslip, β. In addition, the airspeed of the projectile is given by the magnitude of the velocity vector $\vec{V}$ and can be written as

$$V = \sqrt{u^2 + v^2 + w^2}, \tag{7}$$

and the aerodynamic angles can be written in terms of the body-fixed component velocities as

$$\alpha = \arctan\left(\frac{w}{u}\right), \tag{8}$$

$$\beta = \arcsin\left(\frac{v}{V}\right). \tag{9}$$

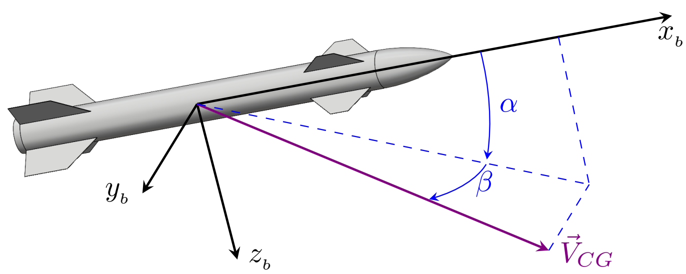

Fig. 3 Wind reference frame relative to the body-fixed reference frame. Angle of attack and angle of sideslip relate to the projectile's center-of-gravity velocity vector.

With the full 6-degree-of-freedom equations of motion defined, we now note the common practice of linearizing and decoupling dynamics into the longitudinal and lateral-directional modes. For the purpose of this report, we consider the short-period mode of the longitudinal dynamics. The short-period mode is described by the dynamics of angle of attack α and pitch rate q. Using Eqs. 5 and 6, along with the appropriate forces and moments, and Eq. 8, the short-period dynamics can be written as

$$\begin{bmatrix} \dot{\alpha} \\ \dot{q} \end{bmatrix} = \begin{bmatrix} \frac{Z_\alpha}{V} & 1 \\ M_\alpha + M_{\dot{\alpha}} \frac{Z_\alpha}{V} & M_q + M_{\dot{\alpha}} \end{bmatrix} \begin{bmatrix} \alpha \\ q \end{bmatrix} + \begin{bmatrix} \frac{Z_{\delta_q}}{V} \\ M_{\delta_q} + M_{\dot{\alpha}} \frac{Z_{\delta_q}}{V} \end{bmatrix} \delta_q. \tag{10}$$

Here, δ_q is the control input for pitch motion, and the terms Z_α, M_α, $M_{\dot{\alpha}}$, M_q, Z_{δ_q}, and M_{δ_q} are dimensional derivatives and given in Table 1 where $Q = \frac{1}{2}\rho V^2$ is the dynamic pressure (ρ being the air density), $S = \frac{\pi}{4} D^2$ is the aerodynamic reference area, and D is the projectile diameter. The stability and derivative coefficients given by C_{Z_α}, C_{m_α}, $C_{m_{\dot\alpha}}$, C_{m_q}, $C_{Z_{\delta_q}}$, and $C_{m_{\delta_q}}$ are obtained from aerodynamic modeling of the forces and moments on the projectile.

Table 1 Dimensional derivative terms

$Z_\alpha = \frac{QS}{m} C_{Z_\alpha}$	$Z_\delta = \frac{QS}{m} C_{Z_{\delta_q}}$
$M_\alpha = \frac{QSD}{I_y} C_{m_\alpha}$	$M_{\dot\alpha} = \frac{QSD}{I_y} \frac{D}{2V} C_{m_{\dot\alpha}}$
$M_q = \frac{QSD}{I_y} \frac{D}{2V} C_{m_q}$	$M_\delta = \frac{QSD}{I_y} C_{m_{\delta_q}}$

Since the control objective will be to follow a desired acceleration command, we note here that the projectile's specific vertical acceleration $A_Z = -F_Z/m$ can be written as

$$A_Z = \begin{bmatrix} -Z_\alpha & 0 \end{bmatrix} \begin{bmatrix} \alpha \\ q \end{bmatrix} + \begin{bmatrix} -Z_{\delta_q} \end{bmatrix} \delta_q, \tag{11}$$

where the negative sign is used by convention so a positive angle of attack supplies a positive vertical acceleration.

4. Tail-Controlled Projectiles are Nonminimum Phase Systems

The flight dynamics presented in the previous section take the form of linear time invariant systems to simplify the analysis, but in reality, the dynamics are highly nonlinear and so the relevant aerodynamic coefficients vary across the flight envelope. Additional internal states may be measurable, but we only consider a single output in our analysis here to maintain a square system, which is one of the requirements of Theorem 1.

4.1 Tail-Controlled Projectile Dynamics without Actuator Dynamics

Letting $x = [\alpha, q]^{\mathrm{T}}$ and $y = A_z$, we write the short-period mode dynamics given by Eqs. 10 and 11 in compact form as

$$\dot{x} = Ax + Bu, \tag{12}$$

$$y = Cx + Du, \tag{13}$$

with

$$A = \begin{bmatrix} \frac{Z_\alpha}{V} & 1 \\ M_\alpha + M_{\dot{\alpha}} \frac{Z_\alpha}{V} & M_q + M_{\dot{\alpha}} \end{bmatrix}, \quad B = \begin{bmatrix} \frac{Z_{\delta_q}}{V} \\ M_{\delta_q} + M_{\dot{\alpha}} \frac{Z_{\delta_q}}{V} \end{bmatrix},$$
$$C = \begin{bmatrix} -Z_\alpha & 0 \end{bmatrix}, \quad D = -Z_{\delta_q},$$

and $u = \delta_q$. The output $y = A_z$ is used because the tail-controlled guidance package generates body acceleration commands $A_{z,\mathrm{CMD}}$. Crucially, notice that Theorem 1 is not applicable here because of the nonzero feedthrough term D. There is some existing literature on the almost strictly dissipative (ASD) conditions for systems with feedthrough terms,[24,25] but a closed form test like that suggested by Theorem 1 does not exist and greatly complicates the analysis.

4.1.1 Sensor Blending Ignoring the Feedthrough Term

We could attempt to ignore the feedthrough term D, treating it as a disturbance if it is small enough. However, when the effect of D is ignored in the short-period dynamics, the remaining dynamics have a single, stable transmission zero as seen in Fig. 4 and are accordingly already minimum phase. This means the sensor blending term will be zero. Thus, we conclude that ignoring the D term for these dynamics prevents the modification of the dynamics to be minimum phase.

4.1.2 Existing Solution for Nonminimum Phase Dynamics

Figure 5 shows the pole-zero map for the dynamics in Eqs. 10 and 11 at a single point in the flight envelope where the airspeed is Mach 2 and $\alpha = 4°$. There are two poles, both of which are stable. Additionally, there are two transmission zeros, one stable and one unstable. It is known that “blending” some amount of q into the output measurement yields a minimum phase plant output.[18] This “blending” can

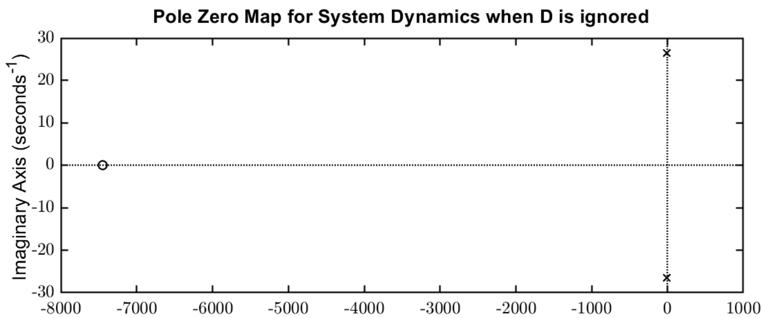

Fig. 4 Pole-zero map for short-period dynamics when feedthrough D term is ignored

be expressed as

$$\tilde{y} = Cx + Du \tag{14}$$

$$\tilde{A}_z = \begin{bmatrix} Z_\alpha & -\Delta C \end{bmatrix} \begin{bmatrix} \alpha \\ q \end{bmatrix} + Z_{\delta_q} \delta_q. \tag{15}$$

From Fig. 6, we see that as more q is blended into the measured output $\tilde{y}$, the unstable transmission zero is stabilized and the system dynamics become minimum phase. This approach makes the modified system dynamics amenable to control ar-

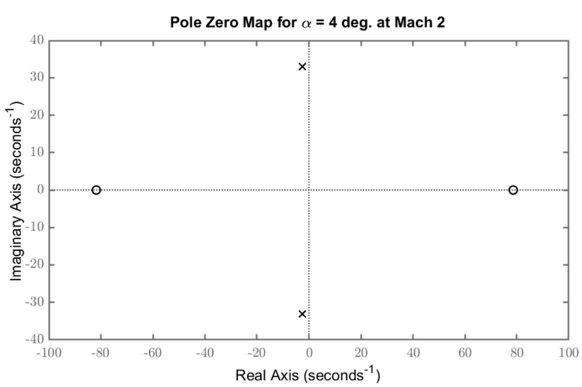

Fig. 5 Pole-zero map for short-period dynamics

chitectures that require minimum phase dynamics, such as dynamic inversion controllers. However, it is sensitive to unmatched uncertainty that may result in oscillations in the actual plant output A_z.[26] Further, the form of Eq. 11 has a nonzero feedthrough term, so Theorem 1 may not be immediately applied to analyze the positive realness of the short-period dynamics. As a result, we turn to a modifica-

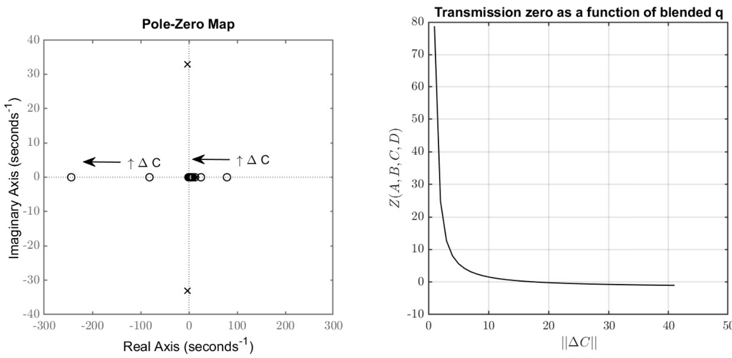

Fig. 6 Blending increasingly more roll q into the output measure makes the system minimum phase

tion of the dynamics in Eq. 10, which includes the body acceleration A_z in the plant state such that there is not a feedthrough term.

4.2 Tail-Controlled Projectile Dynamics with Actuator Dynamics

It is convenient to include A_z as an internal plant state with the representation

$$\begin{bmatrix} \dot{A}_z \\ \dot{q} \\ \dot{\delta}_q \\ \ddot{\delta}_q \end{bmatrix} = \begin{bmatrix} \frac{Z_\alpha}{V} & Z_\alpha & 0 & Z_\delta \\ \frac{M_\alpha}{Z_\alpha} & M_q & M_\delta - \frac{M_\alpha Z_\delta}{Z_\alpha} & 0 \\ 0 & 0 & 0 & 1 \\ 0 & 0 & -\omega^2 & -2\zeta\omega \end{bmatrix} \begin{bmatrix} A_z \\ q \\ \delta_q \\ \dot{\delta}_q \end{bmatrix} + \begin{bmatrix} 0 \\ 0 \\ 0 \\ \omega^2 \end{bmatrix} \delta_q^{\text{CMD}} \tag{16}$$

with the output

$$A_z = \begin{bmatrix} 1 & 0 & 0 & 0 \end{bmatrix} \begin{bmatrix} A_z \\ q \\ \delta_q \\ \dot{\delta}_q \end{bmatrix}. \tag{17}$$

Of course, Eq. 16 is a higher cardinality state space model than Eq. 10. However, it considers some approximations of actuator dynamics and does not have a feedthrough term in the output.

Figure 7 shows the pole-zero plot for the dynamics in Eq. 16 at Mach 3.8 and $\alpha = 12°$. There are two transmission zeros, one of which is unstable. This is a representative linear model whose unstable transmission zeros have the greatest positive real part for all models in the flight envelope. Accordingly, treating this

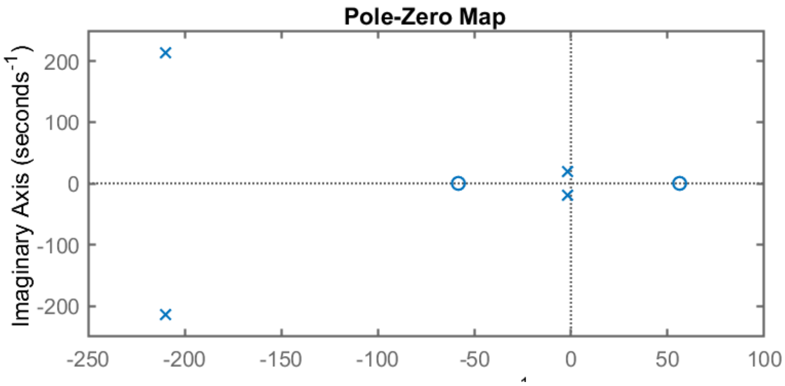

Fig. 7 Pole-zero plot for dynamics at Mach 3.8 and $\alpha = 12°$

case should treat all the linear models in the envelope whose positive real part would be lesser. For the normal form (see the Appendix) to exist, CB must be positive definite. We treat this first. Leaking a small amount of the actuator rate through to the output makes $CB > 0$

$$\tilde{C} = \begin{bmatrix} -1 & 0 & 0 & 0.1 \end{bmatrix}. \tag{18}$$

Accordingly,

$$\tilde{C}B = \begin{bmatrix} -1 & 0 & 0 & 0.1 \end{bmatrix} \begin{bmatrix} 0 \\ 0 \\ 0 \\ \omega^2 \end{bmatrix} = \omega^2/10 \tag{19}$$

which is positive definite. Then, we follow the procedure in the Appendix making use of a state-space transformation to isolate the presently unmeasurable zero dynamics so that they may be included in the output. Interested readers should see Balas and Fuentes[14] for more detail. The state-space transformation results in the following matrices,

$$P_1 = \begin{bmatrix} 0 & 0 & 0 & 0 \\ 0 & 0 & 0 & 0 \\ 0 & 0 & 0 & 0 \\ -10.0 & 0 & 0 & 1.0 \end{bmatrix} \tag{20}$$

$$P_2 = \begin{bmatrix} 1.0 & 0 & 0 & 0 \\ 0 & 1.0 & 0 & 0 \\ 0 & 0 & 1.0 & 0 \\ 10.0 & 0 & 0 & 0 \end{bmatrix} \tag{21}$$

$$A_{22} = \begin{bmatrix} -5.7 & 45.0 & 0.012 \\ 0 & 0 & 1.0 \\ -5.7e+4 & 0 & 76.0 \end{bmatrix} \tag{22}$$

$$\bar{B} = WB = \begin{bmatrix} 9.0e+3 \\ 0 \\ 0 \\ 0 \end{bmatrix} \tag{23}$$

$$\bar{C} = CW^{-1} = \begin{bmatrix} 1.0 & 0 & 0 & 1.4e-17 \end{bmatrix} \tag{24}$$

$$\bar{A} = WAW^{-1} = \begin{bmatrix} -500.0 & 5.6e+3 & -9.0e+3 & -49.0 \\ 0 & -5.7 & 45.0 & 0.012 \\ 10.0 & 0 & 0 & 1.0 \\ 810.0 & -5.7e+4 & 0 & 76.0 \end{bmatrix}. \tag{25}$$

Accordingly, we can arbitrarily select the locations of the transmission zeros. Here, it is of interest to this work to evaluate the minimum possible modification to the C matrix. Recall,

$$Cx = \begin{bmatrix} 1 & 0 & 0 & 0.1 \end{bmatrix} \begin{bmatrix} A_z \\ q \\ \delta_q \\ \dot{\delta}_q \end{bmatrix}. \tag{26}$$

Ideally, we would like to not need feedback from δ_q and $\dot{\delta}_q$. If we can restrict modification of the C matrix to

$$\tilde{C} = C + \begin{bmatrix} \Delta c_{1,1} & \Delta c_{1,2} & 0 & 0 \end{bmatrix}, \tag{27}$$

we would only need currently available measurements and our approach would align with existing results from Hindman and Shell.[6] Note that $\dim \bar{A}_{22} = 3$. From this, we know $\Delta C_2 \in \mathbb{R}^{3\times 1}$. Symbolically, we can evaluate how changes in ΔC_2 impacts C. Denote

$$\Delta C_2 = \begin{bmatrix} c_1 & c_2 & c_3 \end{bmatrix}. \tag{28}$$

Then,

$$\Delta C_2 W2P2 = \begin{bmatrix} \sqrt{101}c_3 & c_1 & c_2 & 0 \end{bmatrix}. \tag{29}$$

Therefore, if we can restrict $c_2 = 0$, we will not require actuator command feedback. Curiously, this zero pole placement approach *cannot* impact the feedback required from the actuator rate $\dot{\delta}_q$.

With state feedback control, linear matrix inequalities (LMIs) can be used to find feedback gains with restrictions on the gain matrix. This problem of zero placement is analogous to full state output feedback where

$$\dot{x} = Ax + Bu = A_{22}x + A_{21}u \tag{30}$$

$$u = -Kx. \tag{31}$$

This generates the algebraic equation

$$(A_{22} - A_{21}K)^* P + P(A_{22} - A_{21}K) < 0,\ P > 0. \tag{32}$$

This equation is a bilinear matrix inequality (BMI), which needs to be formulated as an LMI before we can solve it. The equivalent LMI is realized through a congruence transformation

$$SA_{22}^* + A_{22}S - SK^*A_{21} - A_{21}KS < 0,\ P > 0,\ Z \equiv KS, S \equiv P^{-1} \tag{33}$$

such that $K = ZS^{-1}$. This expression is an LMI and can be solved with any number of LMI solvers (CVX, feasp, etc.).

However, solving this equation in its current form will yield results similar to the previous linear quadratic regulator method. We have not yet treated the restrictions on ΔC_2. The second element c_2 of ΔC_2 is

$$k_2 = ZS^{-1}(1,2) = \frac{-(s_{11}s_{32}z_3 - s_{11}s_{33}z_2 - s_{12}s_{31}z_3 + s_{12}s_{33}z_1 + s_{13}s_{31}z_2 - s_{13}s_{32}z_1)}{(s_{11}s_{22}s_{33} - s_{11}s_{23}s_{32} - s_{12}s_{21}s_{33} + s_{12}s_{23}s_{31} + s_{13}s_{21}s_{32} - s_{13}s_{22}s_{31})}. \tag{34}$$

If we want this fraction to be 0, we can set $z_2 = s_{32} = s_{12} = 0$ and the previous LMI expression is still an LMI. Figure 8 shows the algorithm used in CVX to solve the LMI.

```
cvx_begin sdp

     variable S(3,3) symmetric
     variable Z(1,3)

     S(1,2)==0;
     S(3,2)==0;
     Z(1,2)==0;

     A22*S+S*A22'-A21*Z-Z'*A21' <= -eps.*diag([1 1 1])
     S>= -1.*diag([1 eps eps])

cvx_end

DeltaC2=K2*W2*P2;

eig_sym=eig(A22-A21*K2);

tildeC= LMref.C + K2*W2*P2
```

Fig. 8 Algorithm to solve LMI

This results in

$$\Delta C_{2,\text{CVX}} = \begin{bmatrix} 1.21 & 366 & 0 & 0 \end{bmatrix}, \tag{35}$$

and the modified output

$$\tilde{C} = \begin{bmatrix} 0.21 & 366 & 0 & 0.1 \end{bmatrix}. \tag{36}$$

From Fig. 9, the zeros for all linear models in the flight envelope are stable, not just the fastest ones in the linear model we used to generate $\Delta C_{2,\text{CVX}}$. For further comparison, see Fig. 10 with unstable zeros. This shows the transmission zeros of the original unmodified output across the entire flight envelope.

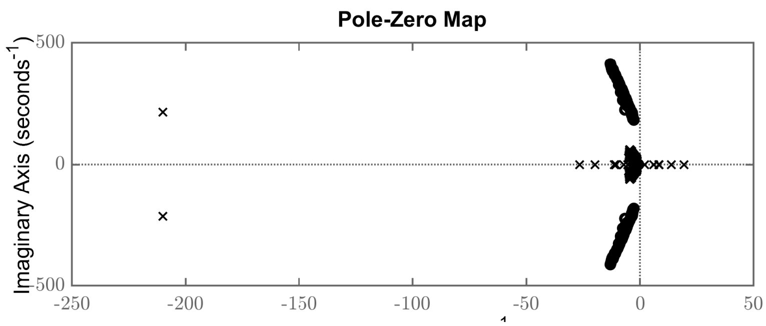

Fig. 9 Pole-zero plot for all linear models in the flight envelope using the redefined output $\tilde{C}$

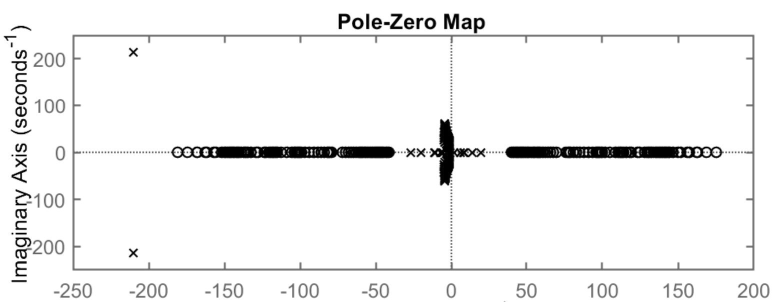

Fig. 10 Pole-zero plot all linear models in the flight envelope using the original output C

The redefined output is minimum phase across the flight envelope and is accordingly amenable to bolt-on adaptive control approaches as shown in the next section.

5. Example: Bolt-on Adaptive Regulator

For this example, we use the redefined output in Eq. 36, and LINLTV.GAQ(:,:,5,5) even though we used the LINLTV.GAQ(:,:,8,17) model to modify the output. We consider the standard adaptive scheme for model reference adaptive control (MRAC) reference command tracking (see Balas et al.[27] for a complete technical treatment)

$$\text{Plant:} \begin{cases} \dot{x} = Ax + Bu, \\ y = Cx, \end{cases} \tag{37}$$

$$
\text{Adaptive Controller: } \begin{cases} u = G_e e_y + G_m x_m + G_u u_m, \\ \dot{G}_e = -e_y e_y^* \sigma_e, \ \sigma_e > 0, \\ \dot{G}_m = -e_y x_m^* \sigma_m, \ \sigma_m > 0, \\ \dot{G}_u = -e_y u_m^* \sigma_u, \ \sigma_u > 0. \end{cases} \tag{38}
$$

Figure 11 shows this scheme graphically. The architecture is particularly well

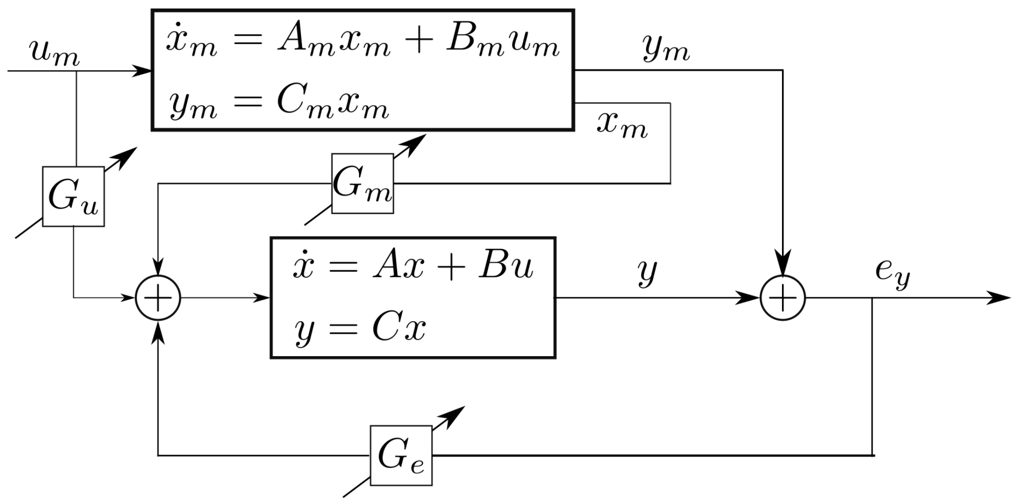

Fig. 11 MRAC architecture

suited to situations where $1 \leq \dim x_m \leq \dim x < \infty$. Note, however, $\dim y_m = \dim y$. All gains $G_e,\ G_m,\ G_u$ are adaptive. For this controller to have stability guarantees, we require

- (A, B, C) minimum phase;
- $Z(A, B, C) \cap (\sigma(A_m) \cup \sigma(F_m)) = \emptyset$;
  - That is, the zeros of the plant (A, B, C) are not shared by the zeros of the reference model.
- $CB > 0$;
- u_m bounded; and
- A_m is stable.

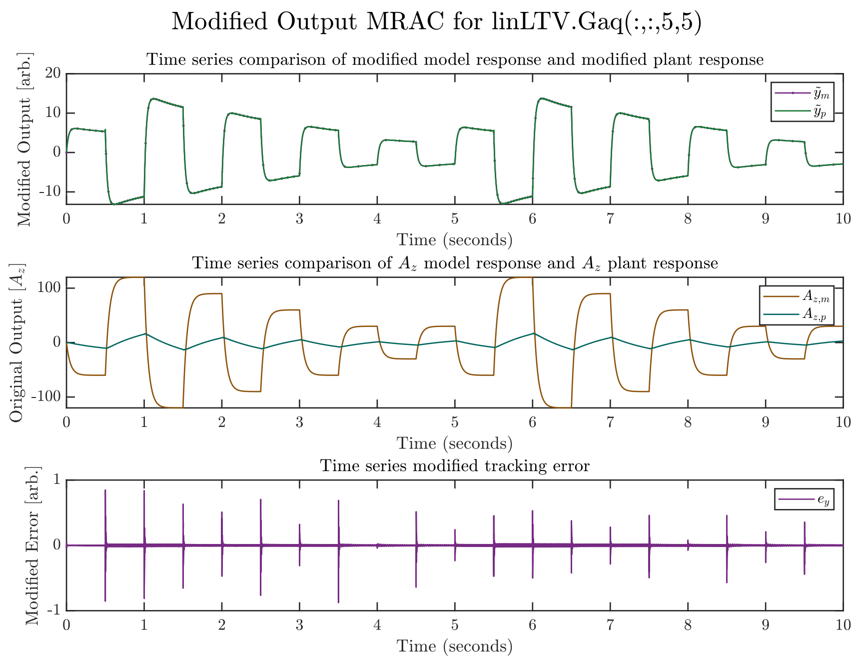

Fig. 12 Modified output MRAC for the 5,5 linear model using the output from Eq. 36

In this bolt-on case, we implement the guidance filter as the reference model. Accordingly,

$$A_m = \frac{-1}{0.05};\ B_m = \frac{1}{0.05};\ C_m = 1. \tag{39}$$

This means the adaptive controller will attempt to track the guidance filter dynamics. Figure 12 shows simulation results for the LINLTV.GAQ(:,:,5,5) using the modified output described previously. While the tracking of the modified output $\tilde{y}$ is acceptable, the actual plant output A_z is poor. The top plot shows that the controller follows the modified output well, while the middle plot shows that this does not translate to good tracking of the A_z command. The modified output contains comparatively less of the A_z dynamics than the other dynamics from $q,\ \delta_q,$ and $\dot{\delta}_q$. If we return to our LMI in Eq. 33 and remove the constraint that c_2 be zero, the CVX algorithm shown in Fig. 13 yields

$$\Delta C_2 = \begin{bmatrix} 240.0 & 78.0 & -0.19 \end{bmatrix} \tag{40}$$

$$\tilde{C} = C + \Delta C_2 W_2 P_2 = \begin{bmatrix} -2.9 & 240.0 & 78.0 & 0.1 \end{bmatrix}. \tag{41}$$

```
cvx_begin sdp

     variable S(3,3) symmetric
     variable Z(1,3)

     A22*S+S*A22'-A21*Z-Z'*A21' <= -eps.*diag([1 1 1])
     S>= -1.*diag([1 eps eps])

cvx_end

DeltaC2=K2*W2*P2;

eig_sym=eig(A22-A21*K2);

tildeC= LMref.C + K2*W2*P2
```

Fig. 13 Modified algorithm to solve LMI

Figure 14 shows simulation results for the LINLTV.GAQ(:,:,5,5) using the modified output in Eq. 41. The top plot shows the controller follows the modified output well, while the middle plot shows this translates to good tracking of the A_z command. This result is more encouraging, even though it requires feedback of the actuator command δ_q. Figure 15 shows simulation results for the LINLTV.GAQ(:,:,8,1) using the modified output described previously. The top plot shows that the controller follows the modified output well, while the middle plot shows that this translates to good tracking of the A_z command. As discussed in the theoretical treatment in the Appendix, this approach is sensitive to how well you can actually reconstruct the modified output. Figure 16 shows the results when we perturb the model $\tilde{C}$, but leave the plant unperturbed. Because the modified output is perturbed, tracking performance of the A_z command is affected, even though we have good tracking of the modified output. The MRAC still tracks the output well, but it is the wrong signal in the physical domain. This suggests a crucial flaw in the sensor blending approach for this system. A second-order approximation of the actuator dynamics is an approximation at best. The control approach presented here is sensitive to how well the actuator command and rate can be blended into the original A_z output. Actuator command and rate feedback is unlikely to be accurate and it is likely to be noisy, so we conclude that sensor blending for the dynamics in Eq. 16 is not an avenue of research worth further pursuit.

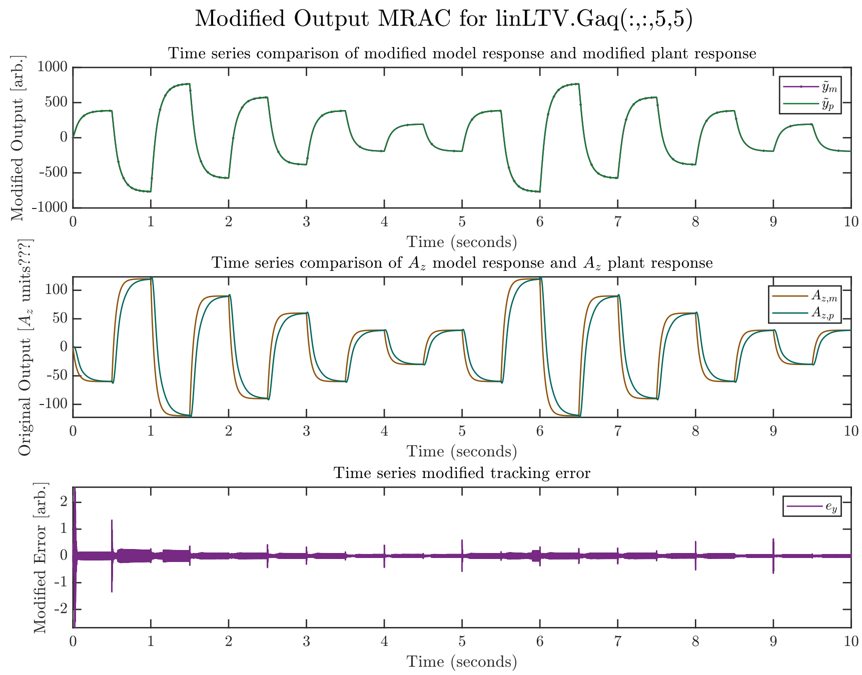

Fig. 14 Modified output MRAC for the 5,5 linear model

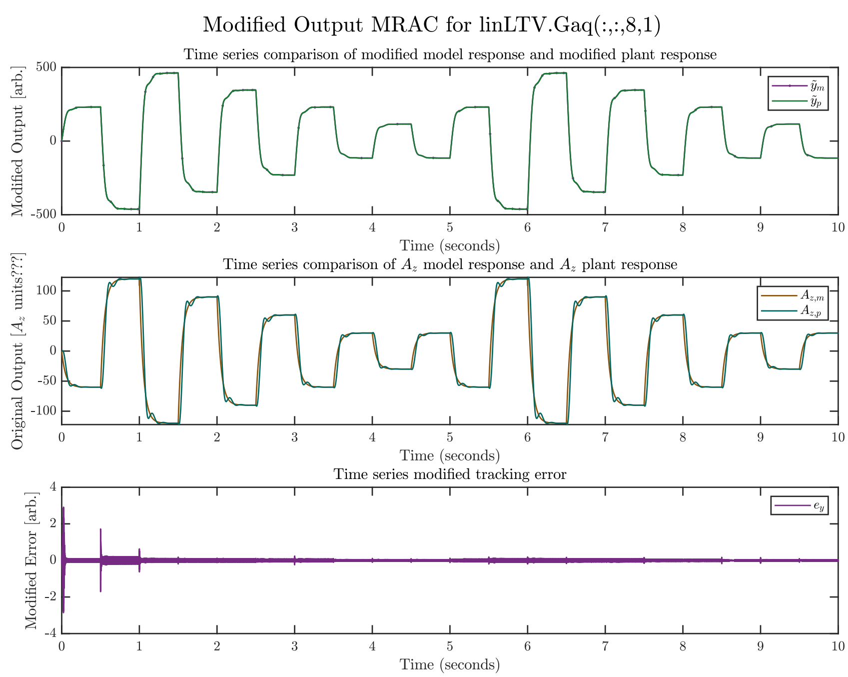

Fig. 15 Modified output MRAC for the 8,1 linear model

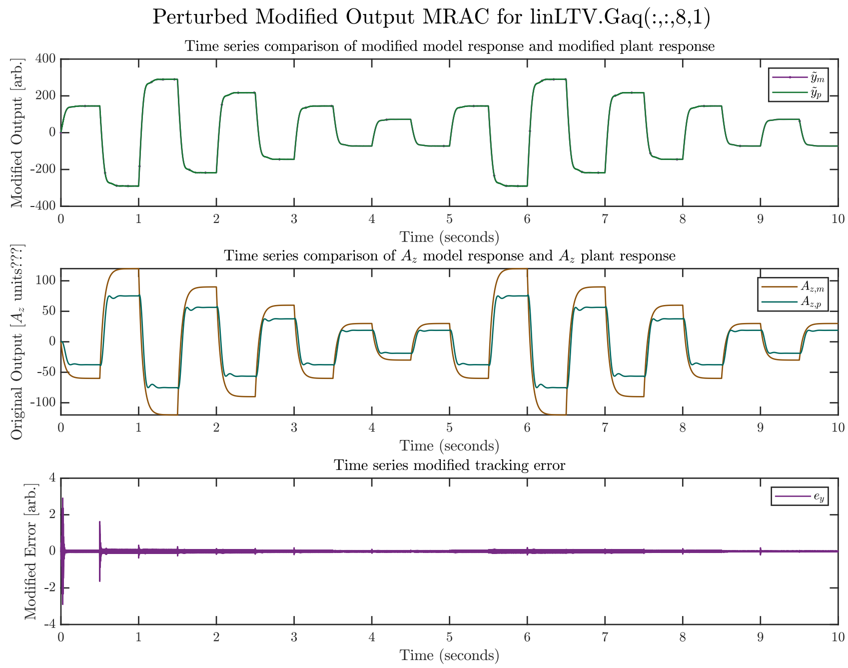

Fig. 16 Modified output MRAC for the 8,1 linear model when there is 20% parametric uncertainty in the modification to C

6. Conclusion

In this work, we established that adaptive controllers are more easily implemented on strictly positive or dissipative systems. Further, it was shown that dynamical systems that can be made strictly dissipative with feedback control are ASD. Adaptive controllers also stabilize on these systems. One of the key requirements of ASD systems is that the transmission (blocking) zeros are in the open left-half plane (stable). Tail-controlled projectiles have unstable transmission zeros across the flight envelope. Therefore, many adaptive and other control techniques are not readily implemented.

From this we developed a survey of existing solutions, a detailed treatment of sensor blending, whereby the plant output is blended with other plant states to stabilize the transmission zeros. This creates a "virtual" output, which may be controlled adaptively through a sensor blending approach for the short-period dynamics stabilizing all the zeros across the flight envelope. A simulation result was presented using the linear models of a tail-controlled projectile with actuator dynamics that leverages the modified output to use MRAC as the controller.

Accordingly, we conclude a modified output is appropriate for the nonminimum phase dynamics, but likely not worth further research pursuit. The only acceptable tracking results were achieved when state feedback from A_z, q, and the actuator states δ_q and $\dot{\delta}_q$ were provided to the controller. Because it is unlikely that all these states, especially the actuator states, be estimated readily, this approach may not be easily implemented for the adaptive control of the example projectile.

7. References

1. Gruenwald BC, Bryson J. Adaptive control for a guided projectile using an expanded reference model. AIAA Scitech 2020 Forum; 2020 Jan. Paper No.: AIAA 2020-1822.

2. Gruenwald BC, Bryson J. Direct uncertainty minimization adaptive control for a guided projectile. AIAA Scitech 2021 Forum; 2021 Jan. Paper No.: AIAA 2021-0783.

3. McFarland M, Hoque S. Robustness of a nonlinear missile autopilot designed using dynamic inversion. AIAA Guidance, Navigation, and Control Conference and Exhibit; 2000 Aug. Paper No.: AIAA-2000-3970.

4. Narendra KS, Annaswamy AM. Stable adaptive systems. Courier Corporation; 2012.

5. Zipfel PH. Modeling and simulation of aerospace vehicle dynamics. American Institute of Aeronautics, Inc.; 2000.

6. Hindman R, Shell WM. Design of a missile autopilot using adaptive nonlinear dynamic inversion. Proceedings of the 2005 American Control Conference; 2005 June. IEEE; 2005. p. 327–332.

7. Peter F, Leitão M, Holzapfel F. Adaptive augmentation of a new baseline control architecture for tail-controlled missiles using a nonlinear reference model. AIAA Guidance, Navigation, and Control Conference; 2012 Jan. Paper No.: AIAA 2012-5037.

8. Brogliato B, Lozano R, Maschke B, Egeland O. Dissipative systems analysis and control. Theory and Applications. 2007;2:2–5.

9. Barmish BR. Necessary and sufficient conditions for quadratic stabilizability of an uncertain system. Journal of Optimization Theory and Applications. 1985;46(4):399–408.

10. Anderson BD, Vongpanitlerd S. Network analysis and synthesis: a modern systems theory approach. Courier Corporation; 2013.

11. Wen JT. Time domain and frequency domain conditions for strict positive realness. IEEE Transactions on Automatic Control. 1988;33(10):988–992.

12. Tao G, Ioannou PA. Necessary and sufficient conditions for strictly positive real matrices. IEE Proceedings G (Circuits, Devices and Systems). 1990;137(5):360–366.

13. Weiss H, Wang Q, Speyer JL. System characterization of positive real conditions. IEEE Transactions on Automatic Control. 1994;39(3):540–544.

14. Balas M, Fuentes R. A non-orthogonal projection approach to characterization of almost positive real systems with an application to adaptive control. Proceedings of the 2004 American Control Conference; 2004 July. Vol. 2. IEEE; p. 1911–1916.

15. Griffith T, Gehlot VP, Balas MJ. Robust adaptive unknown input estimation with uncertain system realization. AIAA Scitech 2022 Forum; 2022 Jan. Paper No.: AIAA 2022-0611.

16. Zelina JK, Prazenica RJ, Henderson T. Adaptive control for nonlinear time-varying rotational systems. AIAA Scitech 2021 Forum; 2021 Jan. Paper No.: AIAA 2021-1120.

17. Gehlot VP, Balas MJ. A theoretical framework for the stable operation of autonomous spacecraft formations in the hill-clohessy-wiltshire frame. 2019 SoutheastCon; 2019 Apr. IEEE; p. 1–7.

18. Siddarth A, Peter F, Holzapfel F, Valasek J. Autopilot for a nonlinear non-minimum phase tail-controlled missile. AIAA Guidance, Navigation, and Control Conference; 2014 Jan. Paper No.: AIAA 2014-1293.

19. Lee HP, Clemens JW, Youssef HM. Dynamic inversion flight control design for aircraft with non-minimum phase response. Aerospace Technology Conference and Exposition; 2011 Oct. SAE International. Paper No.: 2011-01-2617.

20. Barkana I. Extensions in adaptive model tracking with mitigated passivity conditions. Chinese Journal of Aeronautics. 2013;26(1):136–150.

21. Barkana I. Adaptive control? but is so simple! Journal of Intelligent & Robotic Systems. 2016;83(1):3–34.

22. Griffith TD, Zelina J, Bryson JT, Gruenwald BC. Dynamic inversion with adaptive augmentation for a high-speed guided projectile. DEVCOM Army Research Laboratory; 2022 Dec. Report No.: ARL-TR-9620.

23. Bryson J, Gruenwald BC. Automated gain-scheduling approach for three-loop autopilot. DEVCOM Army Research Laboratory; 2022 Sep. Report No.: ARL-TR-9564.

24. Xia M, Antsaklis PJ, Gupta V, McCourt MJ. Determining passivity using linearization for systems with feedthrough terms. IEEE Transactions on Automatic Control. 2015;60(9):2536–2541.

25. Santosuosso GL. Passivity of nonlinear systems with input-output feedthrough. Automatica. 1997;33(4):693–697.

26. Wise K, Lavretsky E, Hovakimyan N. Adaptive control of flight: theory, applications, and open problems. Proceedings of the 2006 American Control Conference; 2006 June. IEEE; 2006. p. 5966–5971.

27. Balas M, Gajendar S, Robertson L. Adaptive tracking control of linear systems with unknown delays and persistent disturbances (or who you callin' retarded?). AIAA Guidance, Navigation, and Control Conference; 2009 Aug. Paper No.: AIAA 2009-5855.

Appendix. Sensor Blending Theory

We abstract our discussion of tail-controlled projectiles and present an overview of sensor blending as a technique to make nonminimum phase systems minimum phase through the use of a redefined output. The treatment that follows relies entirely on Balas and Fuentes[1] and is largely a recreation of that work.

Start with a controllable single input single output (SISO) system. Without loss of generality, consider the dynamics in controllable canonical form:

$$\bar{A} = \begin{bmatrix} 0 & 1 & \dots & 0 \\ 0 & 0 & \dots & 0 \\ 0 & 0 & \dots & 1 \\ -a_0 & -a_1 & \dots & -a_{n-1} \end{bmatrix}, \ \bar{B} = \begin{bmatrix} 0 \\ 0 \\ \vdots \\ 1 \end{bmatrix}, \tag{A-1}$$

$$\bar{C} = \begin{bmatrix} b_0 & b_1 & \dots & b_{N-1} \end{bmatrix}. \tag{A-2}$$

Note that $P(s) = C(sI - A)^{-1}B$ and $CB = \bar{C}\bar{B} = b_{N-1} > 0$. Accordingly, $Z(A, B, C) = Z(\bar{A}, \bar{B}, \bar{C}) = \{\lambda |$ roots of $n(s)$ $\}$.

Can we modify $n(s)$ to have all λ stable such that $P(s)$ is minimum phase (and almost strictly dissipative [ASD])?

A.1 Normal Form

Given the system (A, B, C) that is controllable and observable, $\exists W \equiv \begin{bmatrix} C \\ W_2 P_2 \end{bmatrix}$ such that $W^{-1} = \begin{bmatrix} B(CB)^{-1} & W_2^* \end{bmatrix}$ and

$$\bar{A} = WAW^{-1} = \begin{bmatrix} \bar{A}_{11} & \bar{A}_{12} \\ \bar{A}_{21} & \bar{A}_{22} \end{bmatrix}, \tag{A-3}$$

$$\bar{B} = WB = \begin{bmatrix} CB \\ 0 \end{bmatrix}, \tag{A-4}$$

$$\bar{C} = CW^{-1} = \begin{bmatrix} I & 0 \end{bmatrix}. \tag{A-5}$$

This is a linear transform to an equivalent system where $Z(A, B, C) = \sigma(\bar{A}_{22})$. Now, suppose $\lambda \in \sigma(\bar{A}_{22}))$ is not stable. How can we restore minimum phase?

[1]Balas M, Fuentes R. A non-orthogonal projection approach to characterization of almost positive real systems with an application to adaptive control. Proceedings of the 2004 American Control Conference; 2004 July. Vol. 2. IEEE; p. 1911–1916.

Output feedback or state feedback cannot impact the zero subsystem (see Fig. A-1).

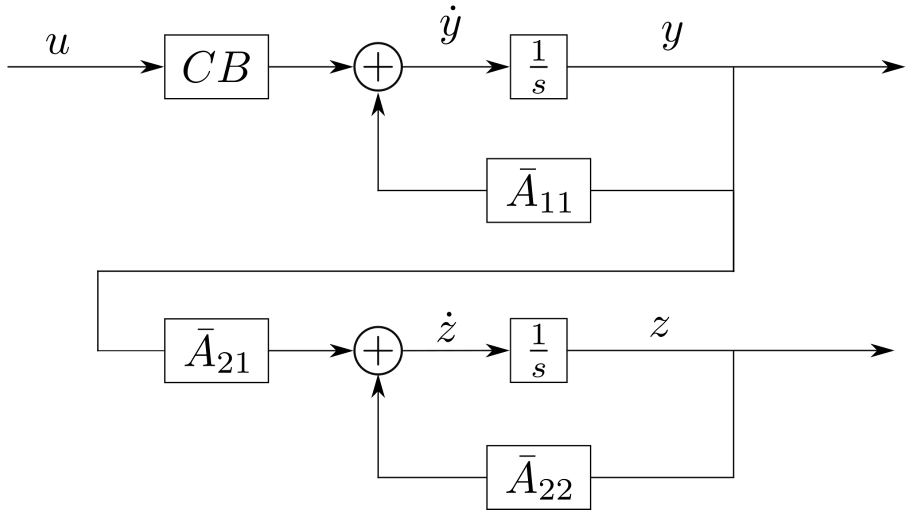

Fig. A-1 Normal form diagram

In equation form, Fig. A-1 can be written as

$$\dot{y} = \bar{A}_{11}y + \bar{A}_{12}z_2 + CBu, \tag{A-6}$$

$$\dot{z}_1 = \bar{A}_{21}y + \bar{A}_{22}z_2. \tag{A-7}$$

It is clear that we must modify the output $y \ni \tilde{y} \equiv y + \Delta\overline{C}_2 z$, where $\Delta\overline{C}_2 z$ is the addition to the output.

Theorem 2. *Let* $\tilde{y} \equiv \widetilde{C}x = (C + \Delta\overline{C}_2 W_2 P_2)x$.

$$Z(A, B, \widetilde{C}) = \sigma(\bar{A}_{22} - \bar{A}_{21}\Delta\overline{C}_2) \tag{A-8}$$

$$\exists\Delta\overline{C}_2 \ni \sigma(\bar{A}_{22} - \bar{A}_{21}\Delta\overline{C}_2) \textit{ is stable,}$$

$$\iff (\bar{A}_{22}, \bar{A}_{21}) \textit{ is a stabilizable subsystem.}$$

From Theorem 2, it follows that finding the correct $\Delta\overline{C}_2$ and adding the sensor blending term $\Delta\overline{C}_2 W_2 P_2 x$ to the output results in the system $(A, B, \widetilde{C})$ being minimum phase. Furthermore, $\widetilde{C}B = CB + \Delta\overline{C}_2 W_2 P_2 B = CB > 0$, and thus, $(A, B, \widetilde{C})$ is ASD.

We leverage three lemmas in this proof.

Lemma 1. *If CB is nonsingular, then $P_1 = B(CB)^{-1}C$ is a (non-orthogonal)* *projection onto the range of B, along the null space of C with $P_2 = I - P_1$ being the complementary projection and $R^n = R(B) \oplus N(C) = R(P_1) \oplus R(P_2)$.*

Proof. Consider

$$P_1^2 = (B(CB)^{-1}C)(B(CB)^{-1}C) = (B(CB)^{-1}C) = P_1, \tag{A-9}$$

so it is a projection. Further

$$R(P_1) \subseteq R(B) \text{ and } z = Bu \in R(B) \tag{A-10}$$
$$\Rightarrow P_1 z = (B(CB)^{-1}C)Bu = Bu = z \in R(P_1) \tag{A-11}$$
$$\therefore R(P_1) = R(B). \tag{A-12}$$

In addition,

$$N(P_1) = N(C) \text{ because } N(C) \subseteq N(P_1) \tag{A-13}$$
$$\text{and } z \in N(P_1) \Rightarrow P_1 z = 0 \Rightarrow CP_1 z = CB(CB)^{-1}Cz = 0 \tag{A-14}$$
$$\therefore N(P_1) \subseteq N(C). \tag{A-15}$$

Accordingly, P_2 is a projection onto $R(B)$ along $N(C)$, but $P_2^* \neq P_2$ so it is not an orthogonal projection. We have $\mathcal{R}^n = R(P_1) \oplus N(P_1)$; hence $\mathcal{R}^n = R(B) \oplus N(C)$. QED

Again, for a detailed proof see Balas and Fuentes.[1] Note that $x = P_1 x + P_2 x$.

Lemma 2. *If CB is nonsingular, there $\exists$ nonsingular $W = \begin{bmatrix} C \\ W_2^* \end{bmatrix} \ni WB = \begin{bmatrix} CB \\ 0 \end{bmatrix}$ and $CW = \begin{bmatrix} I & 0 \end{bmatrix}$. This coordinate transform puts the dynamics into normal form.*

Proof. Consider that

$$y = Cx = C(B(CB)^{-1}C)x = CP_1 x \tag{A-16}$$
$$P_1 x = B(CB)^{-1}Cx = B(CB)^{-1}y. \tag{A-17}$$

In addition,

$$CP_2 = C - CB(CB)^{-1}C = 0 \tag{A-18}$$
$$P_2B = B - B(CB)^{-1}CB = 0. \tag{A-19}$$

Furthermore, we have

$$P_2x = W_2z_2, \tag{A-20}$$

where $z_2 \in R^{n-m}$ and the $n - m$ columns of W_2 form an orthonormal basis for $N(C)$. From this, we have $W_2^*W_2 = I_{n-m}$ and the retraction $z_2 = W_2^*P_2x$. Then, from Lemma 1 we have

$$\begin{aligned}\dot{y} &= CP_1\dot{x}\\ &= CP_1A(P_1x + P_2x) + CP_1Bu\\ &= C(B(CB)^{-1})AB(CB)^{-1}y + C(B(CB)^{-1}C)A(W_2z_2)\\ &\quad + C(B(CB)^{-1}C)Bu\\ &= \bar{A}_{11}y + \bar{A}_{12}z_1 + CBu,\end{aligned} \tag{A-21}$$

and

$$\begin{aligned}\dot{z}_2 &= W_2^*P_x\dot{x}\\ &= W_2^*P_xA(P_1x + P_2x)\\ &= W_2^*P_2A(B(CB)^{-1}y + W_2z_2) + W_2^*P_2Bu\\ &= W_2^*(I - B(CB)^{-1}B)AB(CB)^{-1}y + W_2^*(I - B(CB)^{-1}B)AW_2z_2\\ &= \bar{A}_{11}y + \bar{A}_{22}z_2.\end{aligned} \tag{A-22}$$

This yields the normal form. Choose

$$W \equiv \begin{bmatrix} C \\ W_2^*P_2 \end{bmatrix}. \tag{A-23}$$

Then W has the inverse

$$W^{-1} = \begin{bmatrix} B(CB)^{-1} & W_2 \end{bmatrix}. \tag{A-24}$$

This gives

$$WW^{-1} = I, \tag{A-25}$$

because the columns of W_2 are in $N(C)$ and P_2 projects onto $N(C)$. Finally, $W^{-1}W = P_1 + W_2 W_2^* P_2 = P_1 + P_2 = I$ because $W_2 W_2^*$ is an orthogonal projection onto $N(C)$. By direct calculation

$$\bar{B} \equiv WB = \begin{bmatrix} CB \\ W_2^* P_2 B \end{bmatrix} = \begin{bmatrix} CB \\ 0 \end{bmatrix}, \tag{A-26}$$

$$\bar{C} \equiv CW^{-1} = \begin{bmatrix} CB(CB)^{-1} & CW_2 \end{bmatrix} = \begin{bmatrix} I_m & 0 \end{bmatrix}, \tag{A-27}$$

$$\bar{A} \equiv WAW^{-1} = \begin{bmatrix} CAB(CB)^{-1} & CAW_2 \\ W_2^* P_2 AB(CB)^{-1} & W_2^* P_2 AW_2 \end{bmatrix}. \tag{A-28}$$

QED

Lemma 3. *Assume CB is nonsingular. Define $\bar{A} = WAW^{-1}$, $\bar{B} = WB$, $\bar{C} = CW^{-1}$ where $\bar{A} = \begin{bmatrix} \bar{A}_{11} & \bar{A}_{12} \\ \bar{A}_{21} & \bar{A}_{22} \end{bmatrix}$; then the transmission zeros of (A, B, C) are the eigenvalues of $\bar{A}_{22}$. Consequently,*

- *$\bar{A}_{22}$ is stable if and only if (A, B, C) is minimum phase and*
- *$\bar{A}_{22}$ is weakly stable if and only if (A, B, C) is weakly minimum phase.*

See Balas and Fuentes[1] for further details. Note that by rescaling W with the inverse of CB, the coordinate transformation can produce $\bar{B} = \begin{bmatrix} I_m \\ 0 \end{bmatrix}$ and $\bar{C} = \begin{bmatrix} (CB)^{-1} & 0 \end{bmatrix}$ which greatly simplifies the proofs.

A.2 Illustrative Example

Consider

$$A = \begin{bmatrix} 0 & 1 & 0 \\ 0 & 0 & 1 \\ -1 & -3 & -3 \end{bmatrix}, \quad B = \begin{bmatrix} 0 \\ 0 \\ 1 \end{bmatrix}, \quad C = \begin{bmatrix} 0 & -1 & 1 \end{bmatrix}. \tag{A-29}$$

Accordingly, $\sigma(A) = \{-1,-1,-1\}$ and $Z(A,B,C) = \{0,1\}$ with $CB = 1$. Determine P_1 as follows,

$$P_1 \equiv B(CB)C = BC = \begin{bmatrix}0\\0\\1\end{bmatrix}\begin{bmatrix}0 & -1 & 1\end{bmatrix} = \begin{bmatrix}0 & 0 & 0\\0 & 0 & 0\\0 & -1 & 1\end{bmatrix}. \tag{A-30}$$

Further, we can see that

$$P_2 \equiv I - P_1 = \begin{bmatrix}1 & 0 & 0\\0 & 1 & 0\\0 & -1 & 0\end{bmatrix}. \tag{A-31}$$

$$\therefore \mathcal{N}(C) = \text{sp}\left(\underbrace{\begin{bmatrix}0\\1\\1\end{bmatrix}}_{\phi_1}, \underbrace{\begin{bmatrix}1\\0\\0\end{bmatrix}}_{\phi_2}\right). \tag{A-32}$$

We can then determine W_2 as

$$W_2 = \begin{bmatrix}\phi_1^*\\\phi_2^*\end{bmatrix} = \begin{bmatrix}0 & 1/\sqrt{2} & 1/\sqrt{2}\\1 & 0 & 0\end{bmatrix}, \tag{A-33}$$

$$W_2^* = \begin{bmatrix}\phi_1 & \phi_2\end{bmatrix} = \begin{bmatrix}0 & 1\\1/\sqrt{2} & 0\\1/\sqrt{2} & 0\end{bmatrix}. \tag{A-34}$$

Now, we see

$$W_2P_2 = \begin{bmatrix}0 & \sqrt{2} & 0\\1 & 0 & 0\end{bmatrix}. \tag{A-35}$$

Finally, the matrix W is

$$W \equiv \begin{bmatrix}C\\W_2P_2\end{bmatrix} = \begin{bmatrix}0 & -1 & 1\\0 & \sqrt{2} & 0\\1 & 0 & 0\end{bmatrix}, \tag{A-36}$$

with the inverse

$$W^{-1} \equiv \begin{bmatrix} B(CB)^{-1} \\ W_2^* \end{bmatrix} = \begin{bmatrix} 0 & 0 & 1 \\ 0 & 1/\sqrt{2} & 0 \\ 1 & 1/\sqrt{2} & 0 \end{bmatrix}. \tag{A-37}$$

Now we may perform the coordinate transform into the normal form as

$$\bar{B} = WB = \begin{bmatrix} 1 \\ 0 \\ 0 \end{bmatrix}, \tag{A-38}$$

$$\bar{C} = CW^{-1} = \left[\begin{array}{c|cc} 1 & 0 & 0 \end{array} \right], \tag{A-39}$$

$$\bar{A} = WAW^{-1} = \left[\begin{array}{c|cc} -4 & -7/\sqrt{2} & -1 \\ \hline \sqrt{2} & 1 & 0 \\ 0 & 1/\sqrt{2} & 0 \end{array} \right]. \tag{A-40}$$

Therefore,

$$\bar{A}_{11} = \begin{bmatrix} -4 \end{bmatrix}, \tag{A-41}$$

$$\bar{A}_{12} = \begin{bmatrix} -7/\sqrt{2} & -1 \end{bmatrix}, \tag{A-42}$$

$$\bar{A}_{21} = \begin{bmatrix} \sqrt{2} \\ 0 \end{bmatrix}, \tag{A-43}$$

$$\bar{A}_{22} = \begin{bmatrix} 1 & 0 \\ 1/\sqrt{2} & 0 \end{bmatrix} \Rightarrow \sigma(\bar{A}_{22} = Z(A, B, C) = \{0, 1\}). \tag{A-44}$$

We now have the following,

$$\begin{aligned} \bar{A}_{22} - \bar{A}_{21}\Delta\overline{C}_2 &= \begin{bmatrix} 1 & 0 \\ 1/\sqrt{2} & 0 \end{bmatrix} - \begin{bmatrix} \sqrt{2} \\ 0 \end{bmatrix} \begin{bmatrix} a & b \end{bmatrix} \\ &= \begin{bmatrix} 1 - a\sqrt{2} & -b\sqrt{2} \\ 1/\sqrt{2} & 0 \end{bmatrix}. \end{aligned} \tag{A-45}$$

Letting $a = 6/\sqrt{2}$ and $b = 6$, one can show

$$\det \begin{bmatrix} \lambda + 5 & 6\sqrt{2} \\ -1/\sqrt{2} & \lambda \end{bmatrix} = \lambda^2 + 5\lambda + 6$$

$$= (\lambda + 2)(\lambda + 3), \tag{A-46}$$

which gives $Z(A, B, \widetilde{C}) = \{-2, -3\}$, a stable and minimum phase system.

Therefore, we let $\Delta\overline{C}_2 = \begin{bmatrix} 6/\sqrt{2} & 6 \end{bmatrix}$, which yields

$$\Delta\overline{C}_2 W_2 P_2 = \begin{bmatrix} 6/\sqrt{2} & 6 \end{bmatrix} \begin{bmatrix} 0 & 1/\sqrt{2} & 1/\sqrt{2} \\ 1 & 0 & 0 \end{bmatrix}$$

$$= \begin{bmatrix} 6 & 6 & 0 \end{bmatrix}. \tag{A-47}$$

We then arrive at

$$\widetilde{C} = C + \Delta\overline{C}_2 W_2 P_2$$

$$= \begin{bmatrix} 6 & 5 & 1 \end{bmatrix}, \tag{A-48}$$

which yields the final modified sensing suite

$$A = \begin{bmatrix} 0 & 1 & 0 \\ 0 & 0 & 1 \\ -1 & -3 & -3 \end{bmatrix}, \quad B = \begin{bmatrix} 0 \\ 0 \\ 1 \end{bmatrix}, \quad C = \begin{bmatrix} 6 & 5 & 1 \end{bmatrix}, \tag{A-49}$$

with the minimum phase transfer function

$$P(s) = \frac{6 + 5s + s^2}{1 + 3s + 3s^2 + s^3} = \frac{(s+2)(s+3)}{(s+1)^3}. \tag{A-50}$$

Figure A-2 shows the impulse response of both the original and modified systems. The response of the modified system does not show the patented nonminimum phase down before up behavior seen in the original system.

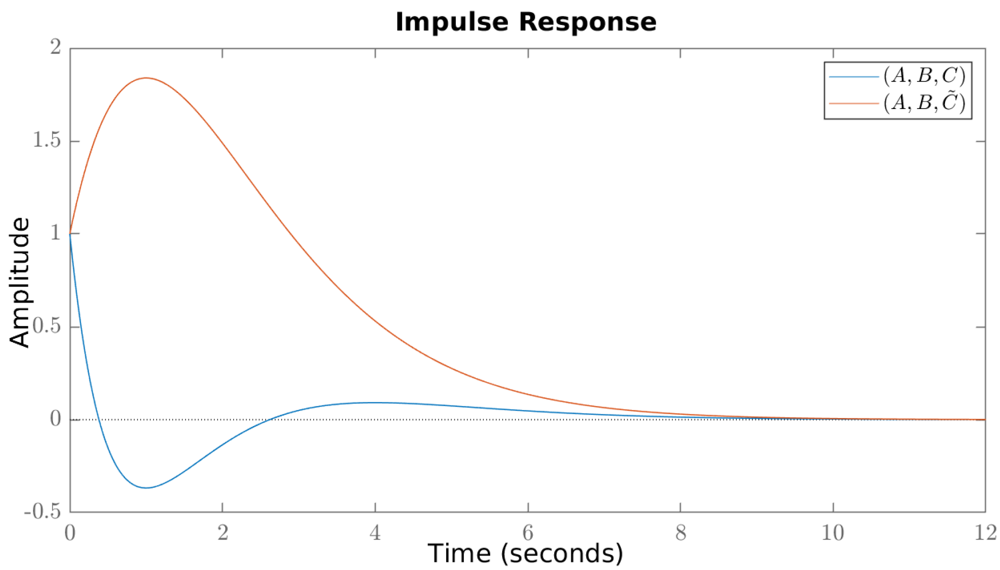

Fig. A-2 Simulating the modified and original impulse responses

List of Symbols, Abbreviations, and Acronyms

aPR	almost positive real
ASD	almost strictly dissipative
aSPR	almost strictly positive real
BMI	bilinear matrix inequality
CG	center-of-gravity
LMI	linear matrix inequality
MRAC	model reference adaptive control
PR	positive real
SISO	single input single output
SPR	strictly positive real

MATHEMATICAL OPERATORS:

$(\dot{\ })$	denotes the time-derivative
$(\vec{\ })$	denotes a vector
$(\cdot)^{\mathrm{T}}$	denotes the transpose operator
$(\times)$	denotes the cross product
$(\cdot)^{-1}$	denotes the inverse operator

1	DEFENSE TECHNICAL
(PDF)	INFORMATION CTR
	DTIC OCA
1	DEVCOM ARL
(PDF)	FCDD RLB CI
	TECH LIB
18	DEVCOM ARL
(PDF)	FCDD RLA CL
	F E FRESCONI
	FCDD RLA W
	T SHEPPARD
	FCDD RLA WD
	J T BRYSON
	B C GRUENWALD
	L STROHM
	B BURCHETT
	I CELMINS
	J DESPIRITO
	L FAIRFAX
	J PAUL
	J D VASILE
	FCDD RLA WA
	N TRIVEDI
	FCDD RLA WB
	J SADLER
	FCDD RLA WC
	M MINNICINO
	FCDD RLA WE
	M ILG
	B TOPPER
	J MALEY
	FCDD RLA WF
	E RIGAS